

# Direct Intracellular Delivery of Cell-Impermeable Probes of Protein Glycosylation by Using Nanostraws

Alexander M. Xu,<sup>[a, b]</sup> Derek S. Wang,<sup>[a]</sup> Peyton Shieh,<sup>[c]</sup> Yuhong Cao,<sup>[a]</sup> and Nicholas A. Melosh<sup>\*[a]</sup>

Bioorthogonal chemistry is an effective tool for elucidating metabolic pathways and measuring cellular activity, yet its use is currently limited by the difficulty of getting probes past the cell membrane and into the cytoplasm, especially if more complex probes are desired. Here we present a simple and minimally perturbative technique to deliver functional probes of glycosylation into cells by using a nanostructured “nanostraw” delivery system. Nanostraws provide direct intracellular access to cells through fluid conduits that remain small enough to minimize cell perturbation. First, we demonstrate that our platform can deliver an unmodified azidosugar, *N*-azidoacetylmannosamine, into cells with similar effectiveness to a chemical modification strategy (peracetylation). We then show that the nanostraw platform enables direct delivery of an azidosugar modified with a charged uridine diphosphate group (UDP) that prevents intracellular penetration, thereby bypassing multiple enzymatic processing steps. By effectively removing the requirement for cell permeability from the probe, the nanostraws expand the toolbox of bioorthogonal probes that can be used to study biological processes on a single, easy-to-use platform.

## Introduction

Metabolic labeling has become an essential tool for tracking the passage and function of biological substrates, yet it is limited by the difficulty of cellular delivery. Early experiments using radiolabeled analogues of glucose and nucleotides allowed researchers to identify downstream biological products in metabolism and DNA replication.<sup>[1,2]</sup> More recently, metabolic labeling has been widely applied to study post-translational modifications (PTMs). PTM types range from small functional-group adornment, such as phosphate and methyl groups, to larger-scale assemblies, such as ubiquitination and glycosylation.<sup>[3,4]</sup> By actively and reversibly modulating protein function,

PTMs are essential for intracellular energy exchange, epigenetic memory, and signal transduction. As the study of PTMs has expanded, so too has the demand for observation of their localization and dynamics, thus driving the search for new functional metabolic analogues.<sup>[5–7]</sup>

Recently, a versatile approach that combines metabolic labeling with bioorthogonal chemistry has emerged.<sup>[8,9]</sup> With this strategy, metabolic analogues bearing a sterically minimized bioorthogonal functional group (“handle”) are delivered into cells. Once in the cytoplasm, the handle is specifically labeled with a fluorophore by bioorthogonal ligation. This method has been especially effective for protein glycosylation studies. Natural glycosylation patterns are among the most complex and variable PTMs, and are composed of many unique monosaccharide subunits attached in linear and branching patterns. Their composition can vary dramatically, and these changes in composition correlate with dramatically altered phenotypes, as evidenced by the altered glycosylation status of cancer cells.<sup>[10]</sup> Bioorthogonal labeling provides the resolution, live-cell compatibility, and multiplexed detection necessary to map the relationship between glycosylation pattern and behavior in cells.<sup>[11,12]</sup>

The key barrier to this flexible labeling scheme is delivery of the metabolic analogues through the cell membrane. Chemical modifications or adjuvants, such as peracetylation<sup>[13,14]</sup> or permeabilizing agents,<sup>[7,15,16]</sup> can improve effectiveness, but these are not universally applicable and can be cytotoxic<sup>[17]</sup> or compromise labeling efficiency. Moreover, the kinetics of enzymatic reactions probed with metabolic analogues are often unknown, and the intracellular levels of a metabolite can require upkeep over several days.<sup>[9]</sup> Unfortunately, most intracellular delivery agents are designed for single-shot delivery of oligonucleotide cargo and are too disruptive to be applied repeatedly, thus making them significantly less effective for consistent, extended metabolic labeling. Without more effective strategies for delivery, the full range of bioorthogonal probes remains untapped, and the delivery of available probes is suboptimal.

Here, we present a simple, nonperturbing technique to deliver poorly membrane-permeable azido-functionalized monosaccharides into cells, where they are incorporated onto glycoproteins and can be labeled by bioorthogonal chemistry.<sup>[18]</sup> This technique uses a nanostructured platform of supported hollow tubes (“nanostraws”) that deliver membrane-impermeable molecules directly into the cytoplasm with minimal cell disruption.<sup>[19–22]</sup> We show that nanostraws enable efficient delivery of *N*-azidoacetylmannosamine (ManNAz) at comparable levels

[a] Dr. A. M. Xu, D. S. Wang, Y. Cao, Prof. N. A. Melosh  
Department of Materials Science and Engineering, Stanford University  
476 Lomita Mall, Stanford, CA 94305 (USA)  
E-mail: nmelosh@stanford.edu

[b] Dr. A. M. Xu  
Present address: Chemistry and Chemical Engineering Division  
California Institute of Technology  
1200 E California Boulevard, Pasadena, CA 91106 (USA)

[c] Dr. P. Shieh  
Department of Chemistry, Stanford University  
333 Campus Drive, Stanford, CA 94305 (USA)

Supporting information and the ORCID identification numbers for the authors of this article can be found under <http://dx.doi.org/10.1002/cbic.201600689>.

to those achieved by chemical modification (peracetylation). More importantly, we show that nanostraws enable the delivery of another metabolite, UDP-*N*-azidoacetylgalactosamine (UDP-GalNAz). This molecule is an intermediate in the glycosylation pathway, yet there is currently no effective strategy for its delivery into cultured mammalian cells. With nanostraw delivery, UDP-GalNAz can act as a carrier for complex functional groups or tags that are incompatible with upstream biosynthetic enzymes. By directly penetrating cells to deliver cargo into the cytoplasm, nanostraws offer a powerful new approach to introduce cell-impermeable bioorthogonal probes for cellular studies. We demonstrate this for azidosugars, but nanostraw delivery is largely agnostic to the cargo, thus enabling generic delivery and unlocking the study of many other biological systems.

## Results and Discussion

Nanostraw membranes are polycarbonate membranes with randomly arranged hollow pores spanning the thickness of the membrane.<sup>[19]</sup> Pores were created with a track-etching procedure for high uniformity along their length and with well-controlled diameters. Following atomic-layer deposition (ALD) of aluminum oxide and two selective etching steps, a forest of nanostraws ( $\sim 3 \times 10^7 \text{ cm}^{-2}$ ) was formed on the membrane. The nanostraws are hollow alumina tubes (100 nm outer diameter, 10 nm wall thickness, 1.5–2  $\mu\text{m}$  length). These tubes are embedded in the polycarbonate polymer substrate (Figure 1), thus making them stable and creating an attractive surface for cell adhesion.

As a result of mechanical interactions, a fraction of the nanostraws will directly penetrate cells cultured onto them,<sup>[21,23]</sup> yet their small size and long leakage pathlength largely limits cell perturbation.<sup>[19]</sup> Penetrant nanostraws act as conduits across

the membrane, thus enabling molecules in solution on one side of the membrane to diffuse through the nanostraws to the other side (Figure 1B). As substrates for cell culture, nanostraws (and related nanowires) are structurally robust and generally non-toxic, although some perturbation in cell behavior has been observed.<sup>[24–26]</sup> Previous applications of nanostraws have included the delivery of small molecules, DNA, membrane impermeable dyes,<sup>[19]</sup> and ions.<sup>[20–21,27]</sup>

For delivery of azidosugars, the nanostraw membranes were assembled into devices consisting of a cell-culture well, an adhesive layer, the nanostraw membrane, and a delivery chamber (Figure 1A, Figure S1A in the Supporting Information). The cell-culture well is a plastic tube (inner diameter,  $\sim 8 \text{ mm}$ ) that holds 300  $\mu\text{L}$  of culture medium, but it can be scaled up or down to accommodate fewer or greater numbers of cells (Figure S1B). The nanostraw membrane, which is uniform over sizes up to several square centimeters, is attached to the culture well with a ring of double-sided, biocompatible tape for the adhesive layer and to provide a water-tight seal. The nanostraw membrane is approximately 20  $\mu\text{m}$  thick and serves as the cell-culture substrate. The delivery chamber is then created with a second ring of double-sided tape to store approximately 20  $\mu\text{L}$  of cargo solution. The assembled device allows cells to be cultured onto the membrane with access to the cargo chamber via the nanostraw conduits. Control experiments used flat membranes with the same pore density but without protruding nanostraws. Reagents to be delivered were pipetted beneath the nanostraw membrane and allowed to diffuse into the cells.

In order to demonstrate delivery of a bioorthogonal chemistry probe into cells through nanostraws we used ManNAz, which results in the introduction of azide groups onto sialylated cell-surface proteins (Figure 1B). Upon incorporation onto surface glycoproteins, the azide moieties of metabolized ManNAz can be specifically labeled with click-chemistry fluorescent probes (fluorophore-conjugated dibenzylcyclooctyne, DBCO). Importantly, a peracetylated derivative of ManNAz ( $\text{Ac}_4\text{ManNAz}$ ), shown to be orders of magnitude more effective in biosynthetic incorporation compared to the parent compound,<sup>[9]</sup> served as a comparison for the efficacy of nanostraw delivery. Cell-permeable  $\text{Ac}_4\text{ManNAz}$  should label cell glycans when presented to cells in solution; the less-permeable ManNAz at the same concentration would require a delivery method such as nanostraws to provide the same labeling. Confirming earlier work, Chinese hamster ovary (CHO) cells incubated for 48 h in control tests in standard 96-well plates with  $\text{Ac}_4\text{ManNAz}$  (100  $\mu\text{M}$ , 10  $\mu\text{M}$  Cy3 DBCO label) showed the characteristic cell-surface fluorescence profile after the bioorthogonal labeling reaction (Figure S2A). However, cells incubated with cell-impermeable ManNAz under identical conditions showed only faint fluorescent staining (Figure S2B).

In order to prepare devices for nanostraw delivery, nanostraw and flat-membrane control devices were prepared by plasma cleaning ( $< 1 \text{ min}$ ) after assembly, followed by overnight UV light exposure and 3 h incubation with 50  $\mu\text{L}$  polylysine or polyornithine (150  $\mu\text{M}$ ). Following three washes in PBS, 100 000 CHO cells were resuspended in DMEM supplemented

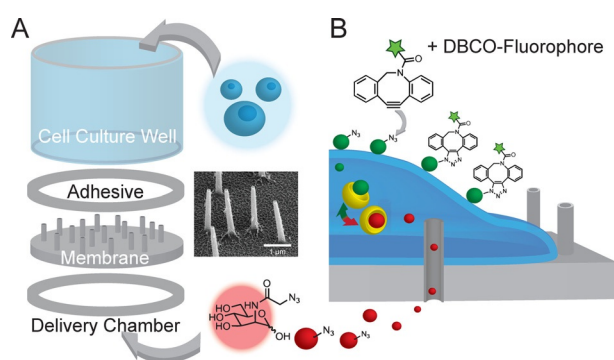


**Figure 1.** Nanostraw device used for azidosugar delivery. A) The device consists of four parts: the cell-culture well, an adhesive layer, the nanostraw membrane, and a delivery chamber. The adhesive produces a water-tight seal between the cell-culture well and the membrane, so that cargo placed in the delivery chamber below can only enter the culture well through the membrane pores. When a nanostraw membrane is used (and the nanostraws have cellular access), the cargo passes directly into cells through penetrating nanostraws. B) Upon successful entry into the cell, an azidosugar such as ManNAz is enzymatically converted into sialic acid groups and incorporated onto cell-surface glycoproteins. These groups retain the azide moiety, which can be specifically labeled with DBCO fluorophore.

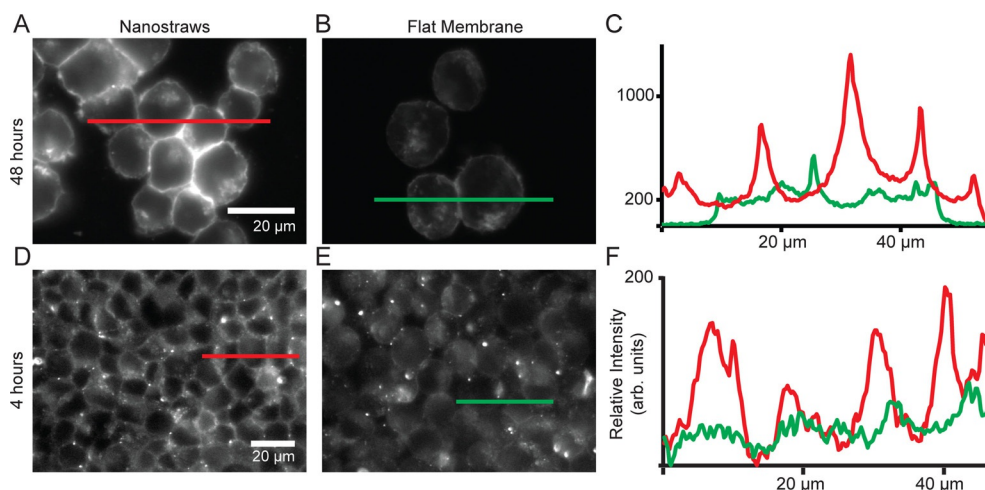


**Figure 2.** ManNAz delivery via nanostraws. A), B) Cells were labeled with Carboxyrhodamine DBCO and imaged after a long-term (48 h) incubation of ManNAz on nanostraw and flat membrane devices. C) Corresponding line traces shows a strong difference in fluorescent intensity between nanostraw delivery and nonspecific uptake. D), E), F) This difference was also evident at 4 h, albeit at reduced intensity.

with 10% FBS and plated on the device. A 20  $\mu$ L drop of ManNAz solution was placed on parafilm, and the device was placed on top to fill the delivery chamber.

Nanostraw delivery of ManNAz was tested for two delivery time scales: long incubation (48 h; Figure 2A–C) and short incubation (4 h; Figure 2D–F). The ManNAz concentration in PBS was either 1 mM (long incubation) or 10 mM (short incubation). After incubation, the medium was removed from the culture chamber, and the delivery chamber was washed in PBS to remove excess ManNAz solution. The culture well was incubated in PBS with 1% FBS for 5 min, rinsed twice with PBS, and incubated in 50  $\mu$ M carboxyrhodamine 110 DBCO or Cy3 DBCO in phenol-red-free DMEM for 15 min at 37  $^{\circ}$ C. Following DBCO incubation, the culture chamber was rinsed three times with PBS, incubated in 0.25% trypsin with EDTA for 10 min, and then the trypsinized cells were replated onto cover slips coated with polylysine. After 4 h to allow cells to adhere, the slides were washed with PBS to remove excess fluorescent label, fixed in 4% paraformaldehyde, and mounted for imaging.

Imaging of cell-impermeable ManNAz delivery after the long incubation (48 h) showed a distinct contrast between the strong DBCO labeling after ManNAz delivery on nanostraw devices (Figure 2A) and the weaker fluorescence on flat membrane devices (Figure 2B). The line profile trace across cells also demonstrates a substantial increase in fluorescence intensity on nanostraw devices relative to flat membrane devices (Figure 2C). Some variations in cell-to-cell fluorescence were observed, as nanostraw-based delivery systems exhibit an inherent spread in cell-to-cell delivery,<sup>[21]</sup> and the nanostraws show markedly increased retention of cells because of improved cell adhesion to nanostraws (and similarly nanowires) during washing.<sup>[28]</sup> A small amount of ManNAz uptake was observed even on flat membrane devices by non-specific uptake mechanisms, but non-specific uptake is unreliable, and the characteristic cell-border fluorescence profile was much weaker.

Images of delivery with the shorter incubation (4 h) revealed that cell-surface labeling had already occurred on nanostraw devices (Figure 2D), in contrast to the indistinct labeling on flat membrane devices (Figure 2E). The difference in raw intensity was less at 4 h than at 48 h (Figure 2F); this is consistent with increased labeling of accumulated azido groups over the longer period.

These results show improved delivery efficiency of poorly permeable azidosugars with nanostraws. Although a peracetylated, cell-permeable ManNAz analogue was available, the true promise of nanostraws lies in facile delivery of metabolites that are difficult (or impossible) to modify chemically. Within this class of metabolites are UDP-modified sugars, which bear a negatively charged diphosphate linkage that limits cell permeability. UDP-sugars are biosynthesized by multiple enzymatic steps from the free monosaccharide for direct attachment onto proteins by glycosyltransferases.<sup>[29]</sup>

Direct delivery of UDP-sugars into the cytoplasm addresses two critical shortcomings. First, by delivering cell-impermeable secondary metabolites (e.g., UDP-sugars) and not their precursors, the activity of specific downstream enzymes within a pathway (here, glycosyltransferases) can be directly probed. Second, although complex functional groups such as UDP groups and fluorophores can be easily attached to free monosaccharides, the resulting modified, bulkier metabolite is often rejected by one or more of the enzymes required for biosynthetic processing and incorporation of the metabolite into the end-product. By directly delivering UDP-sugars into the cytoplasm and bypassing multiple biosynthetic steps, the repertoire of unnatural functionalities to be incorporated onto nascent glycoproteins is freed from the constraints of multiple enzymatic compatibility.

We examined whether nanostraws are effective for a larger variety of unnatural substrates by delivering into GFP-labeled CHO cells three unnatural *N*-acetyl galactosamine derivatives: peracetylated *N*-azidoacetylgalactosamine (Ac<sub>6</sub>GalNAz), *N*-azidoacetylgalactosamine (GalNAz), and the uridine diphosphate



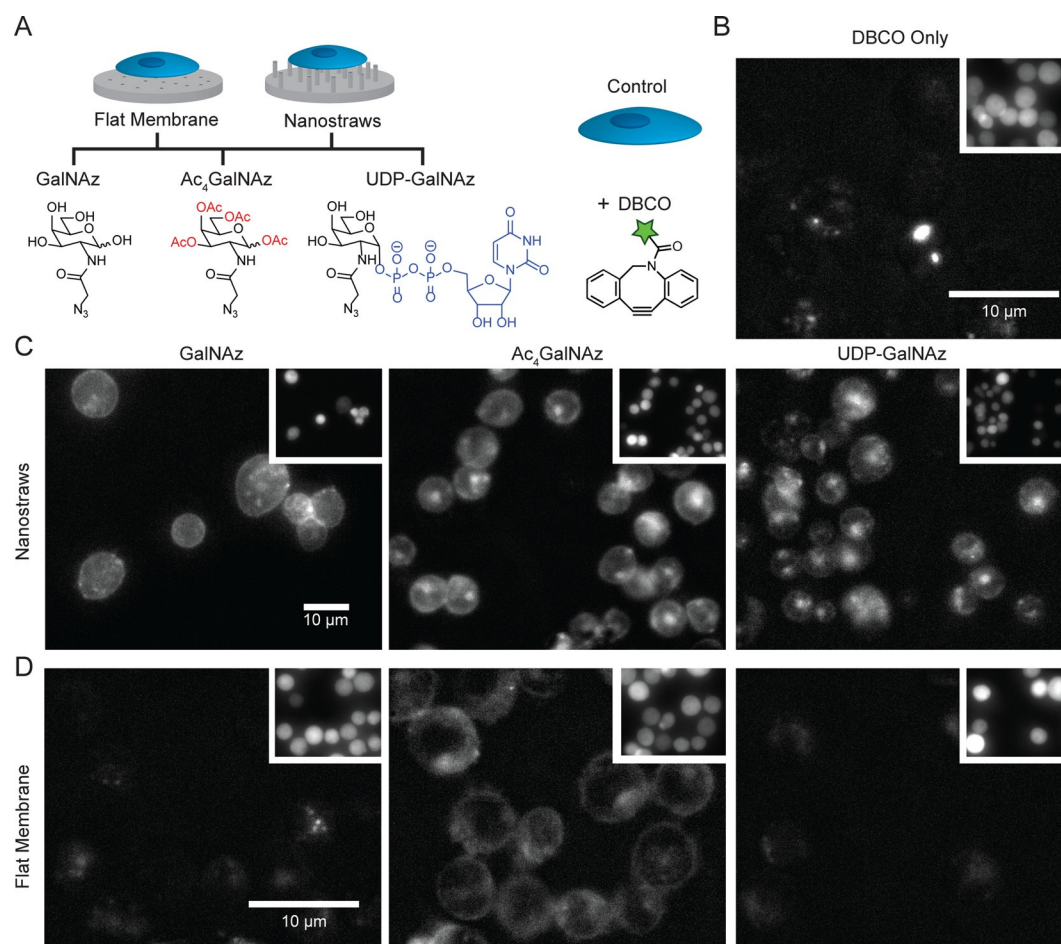


**Figure 3.** Delivery of modified unnatural UDP-sugars. A) Flat membrane and nanostraw delivery were performed with three sugars: GalNAz, Ac<sub>4</sub>GalNAz (cell-permeable), and UDP-GalNAz (negatively charged, cell-impermeable). B) Cells incubated with Cy3 DBCO probes but no azidosugar show some non-specific labeling but not the characteristic cell-border fluorescence (inset: GFP fluorescence). C) When nanostraws were used for delivery, all three forms of GalNAz entered the cells to be incorporated onto surface glycoproteins and labeled. D) On flat control membranes, neither GalNAz nor UDP-GalNAz was delivered into cells; the cell-permeable Ac<sub>4</sub>GalNAz was metabolized and successfully labeled by click chemistry.

modified *N*-azidoacetylgalactosamine (UDP-GalNAz; Figure 3 A). These three molecules can potentially enter the *N*-acetylgalactosamine salvage pathway at different points.<sup>[30]</sup> Although UDP-GalNAz enters at a much later stage than GalNAz, it is significantly less cell-permeable, and its delivery remains a challenge.

We studied the delivery of all three GalNAz sugars through nanostraws and on flat-membrane control devices. For each azidosugar, 500 μM solutions in PBS were added to the delivery chambers, incubated with 50 000 cells for 24 h, then washed and labeled with 10 μM Cy3 DBCO for 20 min. Compared to the negative control (no added azidosugars incubated with DBCO; Figure 3 B, inset: GFP fluorescence), the azidosugars were delivered and labeled with varying success on nanostraws and flat membranes (Figure 3 C–D). Using the nanostraws, all three sugars, including negatively charged and therefore highly impermeable UDP-GalNAz, entered the cells and were transferred onto cell-surface glycoproteins to produce the characteristic cell-border fluorescence upon DBCO labeling (Figure 3 C). GalNAz and Ac<sub>4</sub>GalNAz delivery by nanostraws was nearly 100% efficient in CHO cells and comparable

to ManNAz delivery; UDP-GalNAz delivery was nearly as effective, with only a small number of cells appearing to have weak or no fluorescence.

On flat control membranes, only Ac<sub>4</sub>GalNAz, which is cell-permeable, resulted in fluorescence around cells after DBCO labeling (Figure 3 D). Delivery of both GalNAz and UDP-GalNAz through a flat membrane to cells resulted in only non-specific fluorescence, with a fluorescence profile similar to that for cells with no added sugar (Figure 3 B). For both GalNAz and UDP-GalNAz (and no added sugar control) some fluorescence was observed, likely due to nonspecific uptake of DBCO or labeling of debris. Nanostraws appeared to promote some nonspecific labeling, in the form of bright, central spots of fluorescence, but this was accompanied by circular, cell-border labeling characteristic of bioorthogonal labeling of azido-modified glycoproteins (except in some cases with UDP-GalNAz).

These results show that physical cell penetration and delivery through nanostraws is an effective method to overcome the limitations of cell-impermeable labeling molecules in metabolic labeling studies. Nanostraw delivery of membrane-impermeable ManNAz, a well-characterized molecule for studying

protein glycosylation, reproduced the effect of chemical modification on long- and short-term delivery timescales.

We also demonstrated nanostraw delivery of UDP-GalNAz (an intermediate by-product in GalNAz metabolism), which cannot be delivered by chemical means. The principle of bypassing the cell membrane by nanostraw delivery addresses an essential issue in the application of bioorthogonal probes: that they are potentially poor substrates for the endogenous biosynthetic machinery.<sup>[31]</sup> For natural metabolites that require multiple biosynthetic enzymatic steps, a metabolic analogue that is incompatible with just one enzyme in the pathway will not appear in endogenous biopolymer end-products. In order to bypass such an enzymatic bottleneck, metabolites further downstream in the pathway can be synthesized with the desired bioorthogonal handle. However, these downstream metabolites are naturally processed to be retained in cell compartments, often with charged groups such as UDP, and are therefore poorly cell-permeable, thus requiring an intracellular delivery strategy such as nanostraws.<sup>[32]</sup>

Metabolic analogues that address other pathways of metabolism and post-translational modification are also excellent candidates for nanostraw delivery. These include modified ATP, which can be used in conjunction with modified enzymes to discover new substrates for kinases but suffers from limited delivery options,<sup>[33]</sup> and synthetic cross-linkers or dimerizing agents, which can induce novel interactions in cells to study pathways with increased specificity.<sup>[34]</sup>

Nanostraws represent a minimally perturbative delivery platform capable of delivering a range of freely diffusing species that are effective for sustained delivery over 24 h. The platform can be easily scaled to different numbers of cells by membranes of different size,<sup>[19]</sup> such that larger-scale flow-cytometry quantification or mass spectrometry experiments for proteomics are possible. Finally, nanostraws remove the cell-permeability requirement for chemical probes, thus allowing more diverse and effective chemical probes to be brought to bear on biological problems.

## Experimental Section

**Nanostraw and device fabrication:** Nanostraws were fabricated by using a track-etched membrane template (GVS). The templates were 20  $\mu\text{m}$  thick polycarbonate membranes with randomly arranged pores (density  $3 \times 10^7 \text{ cm}^{-2}$ ). Track-etched membrane templates are generally available only in large volumes at a single prescribed density of extremely thin pores; these are then etched to the desired pore diameter in smaller batches. The nanostraw membranes in this study were etched to 100 nm as purchased. Compared to commercially available track-etched membranes used for water filtration and other applications, the nanostraw membrane templates have relatively low porosity, with either a smaller pore diameter than membranes with similar pore density or a lower density than membranes of similar pore diameter.

Using membranes as purchased, nanostraws were fabricated by coating the templates with ALD alumina. A layer (10–15 nm) of alumina was conformally applied to both sides of the membrane template and to the inner walls of the pores, by using 50 ALD cycles. Each cycle used alternating pulses of trimethylaluminum (TMA)

and  $\text{H}_2\text{O}$  (precursor pulse step, 0.015 s; exposure step, 30 s; purge step, 60 s). The Savannah platform (Cambridge Nanotech/Ultratech, Waltham, MA) accommodates up to 10 cm wafer membranes, and the nanostraws were typically fabricated in smaller-area batches to ensure uniformity. Nanostraws protruding above the membrane were created by first etching one alumina-coated surface of the membrane by an etcher (PlasmaQuest, Hook, UK) with  $\text{BCl}_3$  and  $\text{Cl}_2$  plasma (40 sccm  $\text{BCl}_3$ , 30 sccm  $\text{Cl}_2$ , 5 sccm Ar at 300 W, 250 s) to expose the polycarbonate beneath. The polycarbonate was then removed with an oxygen plasma etch (Plasma Prep III, SPI Supplies, West Chester, PA; 200 mTorr and 100 W, 40 min). The alumina coating the walls of the membrane pores remained to form the free-standing nanostraws.

The device materials consisted of the nanostraw membranes, plastic tubing, and two rings of double-sided tape (3M Acrylic Foam; Digi-key Electronics, Thief River Falls, MN). The double-sided tape was laser cut to form regular rings, and the plastic tubing was polished on both ends to ensure a water-tight seal. For the lower ring of double-sided tape forming the delivery chamber, the plastic covering protecting the lower side of the tape was not removed, in order to prevent the device from sticking to surfaces and to allow access to the delivery chamber to pipette cargo solutions.

**Azidosugar synthesis:** ManNAz,  $\text{Ac}_4\text{ManNAz}$ , GalNAz,  $\text{Ac}_4\text{GalNAz}$ , and UDP-GalNAz were synthesized according to published procedures.<sup>[29, 35]</sup>

**Cell culture and delivery assays:** CHO cells (ATCC, Manassas, VA, USA) and GFP-expressing (Takara, Mountain View, CA, USA) CHO cells for ManNAz and GalNAz experiments, respectively, were cultured in DMEM supplemented with FBS (10%) and penicillin/streptomycin (1%). Prior to cell addition for delivery, the devices were placed in oxygen plasma for sterilization, moved to the tissue-culture hood, and exposed to UV overnight to ensure sterility. Incubation (2–3 h) with polylysine or polyornithine (50  $\mu\text{L}$ ) promoted cell adhesion to the nanostraws. After three wash steps with PBS to remove excess solution, cells were subjected to trypsin (0.25%), re-suspended in DMEM, and added to the cell-culture wells. For the device diameter used here, the delivery chamber stored 20  $\mu\text{L}$  of cargo solution. In order to fill the delivery chamber, a droplet of the solution was placed on parafilm; this prevents the solution from spreading. Slowly placing the device on top of the droplet ensured that air bubbles were minimized. After the delivery chamber was filled, the devices were placed in a humidified Petri dish and returned to the incubator (37 °C). For long-term delivery (> 24 h), it was necessary to replenish the chamber as cargo solution can evaporate.

After incubation, cells were labeled with Cy3 or Carboxyrhodamine DBCO fluorophores (Click Chemistry Tools, Scottsdale, AZ, USA). Cy3 DBCO was used for ManNAz delivery in 96-well plates and GalNAz delivery; carboxyrhodamine DBCO was used for the remaining ManNAz experiments. Excess cargo solution was first washed from the delivery chamber with PBS. Following a short blocking step of the cell-culture chamber with BSA (1% in PBS) and washing (2 $\times$ , PBS), DBCO fluorophores were incubated in the cell-culture chamber for 15 min at 37 °C. After final washing (3 $\times$ , PBS), the cells were prepared for imaging. Because of the small volume of the cell-culture wells and fragility of the nanostraw membrane, thorough washing was difficult. Care was taken to remove as much liquid as possible without puncturing the nanostraw membrane.

For cell imaging, cover slips were prepared by placing a drop of polylysine on the cover slips. After 15 min the cover slips were

washed to remove excess solution. DBCO-labeled and washed cells were resuspended by adding trypsin to the well. Cells cultured on the flat membranes were susceptible to loss during wash steps; nanostraw-adhered cells were trypsinized for longer (5–10 min) to resuspend the cells. After trypsinization, cells were resuspended in medium and added to the cover slips. After 4 h for adherence, the cover slips were washed in PBS to remove excess DBCO fluorophore (necessary because of the washing difficulty described above). Cells were then fixed with paraformaldehyde (4%), mounted on a glass slide, and imaged in an Axiovert 200M confocal microscope (Zeiss) with a Cascade 512B digital camera (Photometrics, Tucson, AZ) and MetaMorph software (Molecular Devices).

## Acknowledgements

We acknowledge HFSP-RGP0048 and Bio-X Interdisciplinary Initiatives Program for support, and A.M.X. support through NSF and NDSEG graduate fellowships. We would like to acknowledge the Sarah Heilshorn Lab and the Stanford Neurofab facility for assisting with microscopy and cell culture access, the David Goldhaber-Gordon and Yi Cui Labs for use of equipment, and the Stanford Nanofabrication Facility and Stanford Nano Shared Facilities for fabrication and imaging.

**Keywords:** click chemistry • drug delivery • fluorescent probes • glycosylation • nanotubes

- [1] M. Reivich, D. Kuhl, A. Wolf, J. Greenberg, M. Phelps, T. Ido, V. Casella, J. Fowler, E. Hoffman, A. Alavi, P. Som, L. Sokoloff, *Circulation Res.* **1979**, *44*, 127–137.
- [2] F. Sanger, S. Nicklen, A. R. Coulson, *Proc. Natl. Acad. Sci. USA* **1977**, *74*, 5463–5467.
- [3] M. Mann, O. N. Jensen, *Nat. Biotechnol.* **2003**, *21*, 255–261.
- [4] Y. L. Deribe, T. Pawson, I. Dikic, *Nat. Struct. Mol. Biol.* **2010**, *17*, 666–672.
- [5] J. Guo, J. Wang, J. S. Lee, P. G. Schultz, *Angew. Chem. Int. Ed.* **2008**, *47*, 6399–6401; *Angew. Chem.* **2008**, *120*, 6499–6501.
- [6] D. H. Dube, C. R. Bertozzi, *Curr. Opin. Chem. Biol.* **2003**, *7*, 616–625.
- [7] J. J. Allen, M. Li, C. S. Brinkworth, J. L. Paulson, D. Wang, A. Hübner, W.-H. Chou, R. J. Davis, A. L. Burlingame, R. O. Messing, C. D. Katayama, S. M. Hedrick, K. M. Shokat, *Nat. Methods* **2007**, *4*, 511–516.
- [8] L. K. Mahal, K. J. Yarema, C. R. Bertozzi, *Science* **1997**, *276*, 1125–1128.
- [9] E. Saxon, C. R. Bertozzi, *Science* **2000**, *287*, 2007–2010.
- [10] A. Varki, R. Kannagi, B. P. Toole in *Essentials of Glycobiology*, 2nd ed. (Eds.: A. Varki, R. D. Cummings, J. D. Esko, H. H. Freeze, P. Stanley, C. R. Bertozzi, G. W. Hart, M. E. Etzler), Cold Spring Harbor Laboratory Press, New York, **2009**.
- [11] P. Shieh, M. S. Siegrist, A. J. Cullen, C. R. Bertozzi, *Proc. Natl. Acad. Sci. USA* **2014**, *111*, 5456–5461.
- [12] B. R. Martin, B. F. Cravatt, *Nat. Methods* **2009**, *6*, 135–138.
- [13] A. K. Sarkar, T. A. Fritz, W. H. Taylor, J. D. Esko, *Proc. Natl. Acad. Sci. USA* **1995**, *92*, 3323–3327.
- [14] S. O. Doronina, B. A. Mendelsohn, T. D. Bovee, C. G. Cervený, S. C. Alley, D. L. Meyer, E. Oflazoglu, B. E. Toki, R. J. Sanderson, R. F. Zabinski, A. F. Wahl, P. D. Senter, *Bioconjugate Chem.* **2006**, *17*, 114–124.
- [15] R. Xie, S. Hong, L. Feng, J. Rong, X. Chen, *J. Am. Chem. Soc.* **2012**, *134*, 9914–9917.
- [16] R. Xie, L. Dong, Y. Du, Y. Zhu, R. Hua, C. Zhang, X. Chen, *Proc. Natl. Acad. Sci. USA* **2016**, *113*, 5173–5178.
- [17] J. B. Haun, N. K. Devaraj, B. S. Marinelli, H. Lee, R. Weissleder, *ACS Nano* **2011**, *5*, 3204–3213.
- [18] B. Belardi, A. de la Zerda, D. R. Spiciari, S. L. Maund, D. M. Peehl, C. R. Bertozzi, *Angew. Chem. Int. Ed.* **2013**, *52*, 14045–14049; *Angew. Chem.* **2013**, *125*, 14295–14299.
- [19] J. J. VanDersarl, A. M. Xu, N. A. Melosh, *Nano Lett.* **2012**, *12*, 3881–3886.
- [20] A. Aalipour, A. M. Xu, S. Leal-Ortiz, C. C. Garner, N. A. Melosh, *Langmuir* **2014**, *30*, 12362–12367.
- [21] A. M. Xu, A. Aalipour, S. Leal-Ortiz, A. H. Mekhdjian, X. Xie, A. R. Dunn, C. C. Garner, N. A. Melosh, *Nat. Commun.* **2014**, *5*, 3613.
- [22] X. Xie, A. M. Xu, S. Leal-Ortiz, Y. Cao, C. C. Garner, N. A. Melosh, *ACS Nano* **2013**, *7*, 4351–4358.
- [23] X. Xie, A. M. Xu, M. R. Angle, N. Tayebi, P. Verma, N. A. Melosh, *Nano Lett.* **2013**, *13*, 6002–6008.
- [24] R. Elnathan, M. Kwiat, F. Patolsky, N. H. Voelcker, *Nano Today* **2014**, *9*, 172–196.
- [25] S. Bonde, N. Buch-Månson, K. R. Rostgaard, T. K. Andersen, T. Berthing, K. L. Martinez, *Nanotechnology* **2014**, *25*, 362001.
- [26] C. N. Prinz, *J. Phys. Condens. Matter* **2015**, *27*, 233103.
- [27] A. M. Xu, S. A. Kim, D. S. Wang, A. Aalipour, N. A. Melosh, *Lab Chip* **2016**, *16*, 2434–2439.
- [28] Y.-R. Na, S. Y. Kim, J. T. Gaub, A. K. Shalek, M. Jorgolli, H. Park, E. G. Yang, *Nano Lett.* **2013**, *13*, 153–158.
- [29] H. C. Hang, C. Yu, M. R. Pratt, C. R. Bertozzi, *J. Am. Chem. Soc.* **2004**, *126*, 6–7.
- [30] J. M. Baskin, K. W. Dehnert, S. T. Laughlin, S. L. Amacher, C. R. Bertozzi, *Proc. Natl. Acad. Sci. USA* **2010**, *107*, 10360–10365.
- [31] M. E. Tanner, *Bioorg. Chem.* **2005**, *33*, 216–228.
- [32] P. Agarwal, B. J. Beahm, P. Shieh, C. R. Bertozzi, *Angew. Chem. Int. Ed.* **2015**, *54*, 11504–11510; *Angew. Chem.* **2015**, *127*, 11666–11672.
- [33] M. R. Banko, J. J. Allen, B. E. Schaffer, E. W. Wilker, P. Tsou, J. L. White, J. Villén, B. Wang, S. R. Kim, K. Sakamoto, S. P. Gygi, L. C. Cantley, M. B. Yaffe, K. M. Shokat, A. Brunet, *Mol. Cell* **2011**, *44*, 878–892.
- [34] K. M. Sakamoto, K. B. Kim, A. Kumagai, F. Mercurio, C. M. Crews, R. J. Deshaies, *Proc. Natl. Acad. Sci. USA* **2001**, *98*, 8554–8559.
- [35] S. T. Laughlin, C. R. Bertozzi, *Nat. Protocols* **2007**, *2*, 2930–2944.

Manuscript received: December 21, 2016

Accepted Article published: January 28, 2017

Final Article published: March 14, 2017